

A NON-CONFORMING ELEMENT FOR STRESS ANALYSIS

ROBERT L. TAYLOR

Department of Civil Engineering, University of California, Berkeley, California, U.S.A.

PETER J. BERESFORD

Dames and Moore, London, England

EDWARD L. WILSON

Department of Civil Engineering, University of California, Berkeley, California, U.S.A.

INTRODUCTION

In this note we wish to comment on properties of some non-conforming elements for plane and three-dimensional stress analysis. In a recent paper¹ a non-conforming element, called Q6, was introduced and applied to some problems where the elements were, in general, parallelograms. Subsequently it was discovered that the Q6 element passes the patch test² only when it is a parallelogram (and does not always pass the patch test for axisymmetric problems even when it is a rectangle). This implies that the element will produce a convergent sequence of solutions only if the mesh subdivisions converge to a set of parallelograms. Such will be the case, for example, when mesh subdivisions are constructed by bisections.

It is possible to 'repair' the defect in the element by examining the patch test and correcting the defective terms. The element which is produced is herein called QM6 and degenerates to the Q6 element whenever it is a parallelogram. To demonstrate the properties of the element the solutions to some example problems are included.

Formulation for non-conforming elements

We take as the basis for constructing a finite element approximation the principle of minimum potential energy which is expressed by:

$$\pi(\mathbf{u}) = \frac{1}{2} \int_V \boldsymbol{\varepsilon}^T \mathbf{D} \boldsymbol{\varepsilon} dV - \int_V \rho \mathbf{f}^T \mathbf{u} dV - \int_{\partial V_t} \hat{\mathbf{t}}^T \mathbf{u} dS = \min \quad (1)$$

where $\boldsymbol{\varepsilon}$ is the strain tensor, \mathbf{u} is the displacement vector, \mathbf{D} is the elasticity tensor, \mathbf{f} is the body force vector, and $\hat{\mathbf{t}}$ is the specified traction vector. In addition, V is the domain of the problem to be solved and ∂V_t is that part of the boundary where tractions are known. The strain tensor is defined in terms of the displacement vector as

$$2\boldsymbol{\varepsilon} = \nabla \mathbf{u} + (\nabla \mathbf{u})^T \quad (2)$$

where ∇ is the gradient operator.

In the finite element method we construct approximate solutions to (1) by dividing V and the boundary ∂V into elements and approximating the displacement vector by interpolations in each element. For the non-conforming elements considered here we start from the 4-point

Received 6 September 1975

isoparametric quadrilateral or the 8-point isoparametric brick element. In the subsequent developments we consider only the plane case (4-point Q4 quadrilateral); the three-dimensional case being obvious.

The isoparametric interpolations for the two-dimensional Q4 element are given by

$$\begin{aligned} \mathbf{u} &= \sum_{i=1}^4 \mathbf{u}_i N_i(s, t) \\ \mathbf{x} &= \sum_{i=1}^4 \mathbf{x}_i N_i(s, t) \end{aligned} \quad (3)$$

where

$$N_i(s, t) = \frac{1}{4}(1 + s_i s)(1 + t_i t) \quad (4)$$

In the above s, t are the natural co-ordinates for the element as shown in Figure 1. The s_i, t_i are the values of s, t at node i . We now add to the dependent variables the two non-conforming

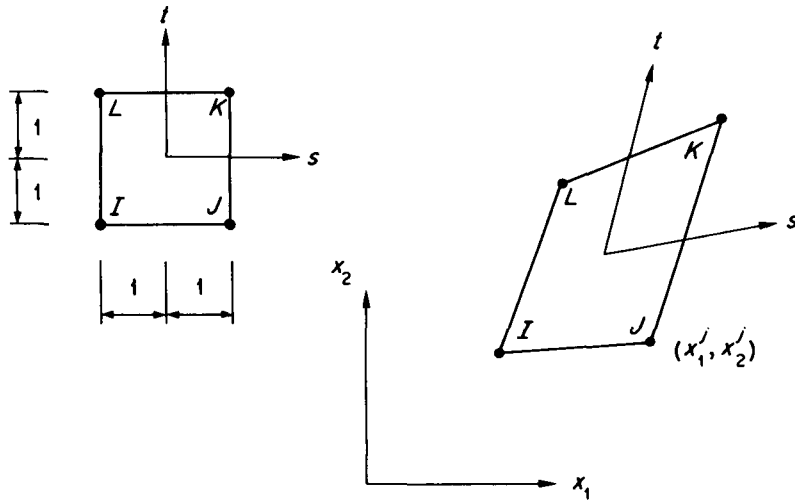


Figure 1. Typical 4-point isoparametric element

modes as described in Reference 1. Accordingly, the dependent variable approximation becomes

$$\mathbf{u} = \sum_{i=1}^4 \mathbf{u}_i N_i(s, t) + \sum_{i=1}^2 \mathbf{a}_i P_i(s, t) \quad (5)$$

where

$$P_1(s, t) = (1 - s^2) \quad \text{and} \quad P_2(s, t) = (1 - t^2) \quad (6)$$

In approximating (1) we use (5) only to describe strain terms, otherwise we use (3). Inserting (5) into (2) for the case of plane deformation we may write

$$\begin{Bmatrix} \epsilon_{11} \\ \epsilon_{22} \\ 2\epsilon_{12} \end{Bmatrix} = \sum_{i=1}^4 [B_i] \begin{Bmatrix} u_{1i} \\ u_{2i} \end{Bmatrix} + \sum_{i=1}^2 [G_i] \begin{Bmatrix} a_{1i} \\ a_{2i} \end{Bmatrix} \quad (7)$$

where

$$[B_i] = \begin{bmatrix} N_{i,1} & 0 \\ 0 & N_{i,2} \\ N_{i,2} & N_{i,1} \end{bmatrix} \quad (8)_1$$

and

$$[G_i] = \begin{bmatrix} P_{i,1} & 0 \\ 0 & P_{i,2} \\ P_{i,2} & P_{i,1} \end{bmatrix} \quad (8)_2$$

We now compute the element stiffness and load matrices and obtain

$$\begin{bmatrix} \mathbf{K}_{uu} & \mathbf{K}_{ua} \\ \mathbf{K}_{au} & \mathbf{K}_{aa} \end{bmatrix} \begin{Bmatrix} \mathbf{u}_0 \\ \mathbf{a}_0 \end{Bmatrix} = \begin{Bmatrix} \mathbf{F}_u \\ \mathbf{0} \end{Bmatrix} \quad (9)$$

where $\mathbf{u}_0, \mathbf{a}_0$ are the set of nodal $\mathbf{u}_i, \mathbf{a}_i$ on the element and

$$[K_{uu}]_{ij} = \int_{V^e} [B_i]^T [D] [B_j] dV \quad (10)_1$$

$$[K_{ua}]_{ij} = \int_{V^e} [B_i]^T [D] [G_j] dV = [K_{au}]_{ji} \quad (10)_2$$

$$[K_{aa}]_{ij} = \int_{V^e} [G_i]^T [D] [G_j] dV \quad (10)_3$$

and

$$\{F_u\}_i = \int_{V^e} N_i \{f\} dV + \int_{\partial V^e} N_i \{\hat{t}\} dS \quad (10)_4$$

For this element to pass the patch test we require \mathbf{a}_0 to be zero whenever \mathbf{u}_0 corresponds to rigid body motions or constant strain conditions. If we define \mathbf{v}_0 as the set of nodal displacements which correspond to one of the above cases, then \mathbf{a}_0 can be computed from the second set of equations in (9). Accordingly,

$$\{a_0\} = -[K_{aa}]^{-1} [K_{au}] \{v_0\} \quad (11)$$

and the requirement for the patch test to be satisfied is for \mathbf{a}_0 to be zero. Examining the right hand side with $[K_{aa}]$ positive definite, \mathbf{a}_0 will be zero only if $[K_{au}] \{v_0\}$ vanishes. We note that

$$[K_{au}] \{v_0\} = \int_{V^e} [G]^T [D] [B] \{v_0\} dV \quad (12)$$

From the assumptions on \mathbf{v}_0 we observe that the term $[D] [B] \{v_0\}$ is in fact some constant stress state $\{\sigma\}$, consequently, the requirement for the patch test to be satisfied reduces to

$$\int_{V^e} [G] dV = \mathbf{0} \quad (13)$$

Using (3)₂, (4), (6) and (8)₂ we can write (13) for each P_i as

$$\int_{V^e} [G_1] dV = 2 \int_{-1}^1 \int_{-1}^1 \begin{bmatrix} -sx_{2,t} & 0 \\ 0 & sx_{1,t} \\ sx_{1,t} & -sx_{2,t} \end{bmatrix} ds dt \quad (14)_1$$

and

$$\int_{V^e} [G_2] dV = 2 \int_{-1}^1 \int_{-1}^1 \begin{bmatrix} tx_{2,s} & 0 \\ 0 & -tx_{1,s} \\ -tx_{1,s} & tx_{2,s} \end{bmatrix} ds dt \quad (14)_2$$

Noting that

$$\begin{aligned} x_{,s} &= \sum_{i=1}^4 x_i s_i (1 + t_i t) \\ x_{,t} &= \sum_{i=1}^4 x_i t_i (1 + s_i s) \end{aligned} \quad (15)$$

we observe that in general (14) will not be zero and that the Q6 element does not pass the patch test. Whenever the element is a parallelogram, however, (15) will consist of constants. In this case the right hand side of (14) will integrate to zero and the patch test will be passed. These results are also confirmed by numerical experiments with the patch test as shown below.

We propose to repair the defect in the non-conforming element and force satisfaction of the patch test. It is generally acknowledged that any element which passes the patch test is a convergent element provided no zero energy modes are contained in a mesh which is restrained against rigid body motions. The proposed remedy consists of replacing in (14) the constant values of (15) computed at s, t zero. These are the values which occur naturally when the element is a parallelepiped, consequently, in this case the element reduces to the one described in Reference 1. This modification is also made to all other terms where the array $[G]$ appears. The justification of such an *ad hoc* change can only be made on the basis of further numerical experiments. Some results on patch tests and sample problems considered in References 3, 4 are presented in the next section.

Example problems

We first consider a patch test for a plane stress problem modelled by the two mesh configurations shown in Figure 2. We apply to the right end consistent nodal loads equivalent to a pure axial normal stress of unit intensity. The exact solution to this problem for $E = 1$ and $\nu = 0.25$ is $u_1 = x_1$ and $u_2 = -x_2/4$. In the patch test experiments we consider the Q4, Q6 and QM6 elements and report in Table I the stresses and displacements for the points labelled in Figure 2. It should be noted that both the Q4 and QM6 elements pass this patch test at all points while the Q6 element passes the patch test only for the mesh of rectangular elements. We next consider a linear varying normal stress with magnitude x_2 as shown in Figure 2 on edge ab ; we also impose antisymmetry boundary conditions to the nodes along edge ac . This corresponds to a pure bending test with solution $u_1 = x_1 x_2$ and $u_2 = -\frac{1}{2}((x_1)^2 - \nu(x_2)^2)$. The finite element solutions for each mesh are shown in Table I.

The results from the above tests show conclusively the failure of the Q6 element to pass the patch test, while both the Q4 and QM6 elements satisfy the tests. Further, the bending experi-

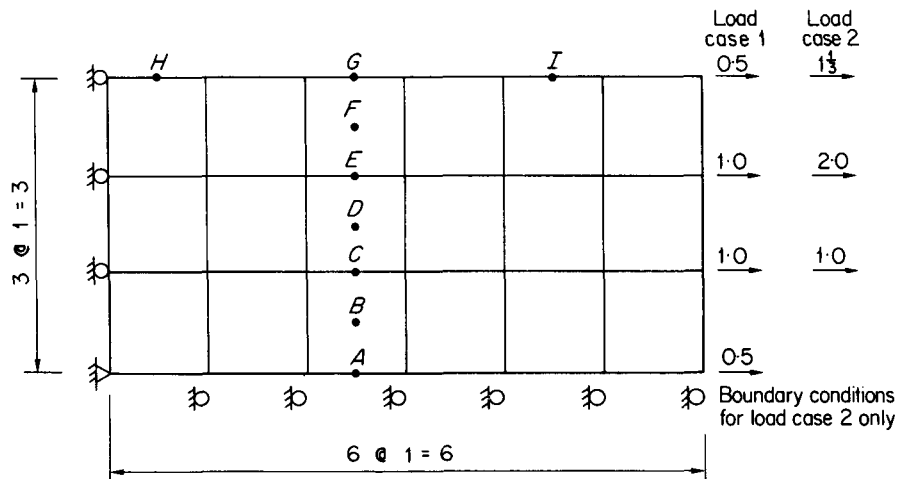


Figure 2(a). Mesh configuration for patch test

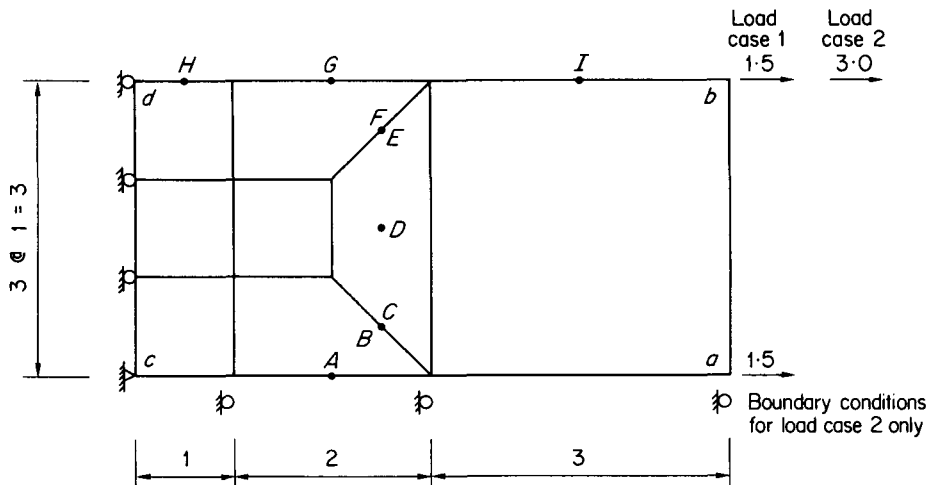


Figure 2(b). Mesh configuration for patch test

ments show that for a mesh with parallelogram elements only the Q6 and QM6 elements are truly higher order (quadratic) elements while having global connections corresponding to the Q4 element. Thus, the global stiffness matrix can be maintained at the same size and bandwidth as the Q4 element, whereas, if 8-node isoparametric elements were used with the same total number of elements both the number of equations and bandwidth would be significantly larger.

As a second example we consider the one element plane stress cantilever beam problem considered in References 3, 4. The properties and loads are shown in Figure 3. The solution to these problems is given in Table II for the points shown in Figure 3 (which are the points considered in Reference 4). The results of the QM6 are compared to those of the Q4 and C5ML from Reference 4. Again it is clear that the QM6 is superior to other elements. In particular it

Table I. (i) Patch test results for mesh shown in Figure 2(a)

Element	A	B	C	D	E	F	G	H	I
Q4	1.000	1.000	1.000	1.000	1.000	1.000	1.000	1.000	1.000
Q6, QM6	1.000	1.000	1.000	1.000	1.000	1.000	1.000	1.000	1.000

(a) Axial loading results—load case 1

Element	A	B	C	D	E	F	G	H	I
Q4	-0.033	0.494	0.988	1.481	1.975	2.468	2.994	2.995	2.975
Q6, QM6	0.000	0.500	1.000	1.500	2.000	2.500	3.000	3.000	3.000
Exact	0.000	0.500	1.000	1.500	2.000	2.500	3.000	3.000	3.000

(b) Bending load results—load case 2

Element	$u_1(a)$ —axial	$u_2(a)$ —bending
Q4	6.000	-17.77
Q6, QM6	6.000	-18.00
Exact	6.000	-18.00

(c) Displacement at tip—point a on Figure 2(a)

Table I. (ii) Patch test results for mesh shown in Figure 2(b)

Element	A	B	C	D	E	F	G	H	I
Q4	1.000	1.000	1.000	1.000	1.000	1.000	1.000	1.000	1.000
Q6	1.342	1.238	-0.953	1.963	-0.953	1.238	1.348	0.924	1.000
QM6	1.000	1.000	1.000	1.000	1.000	1.000	1.000	1.000	1.000
Q6*	1.423	1.152	0.918	0.918	0.918	1.152	1.423	0.924	1.000
QM6*	1.000	1.000	1.000	1.000	1.000	1.000	1.000	1.000	1.000

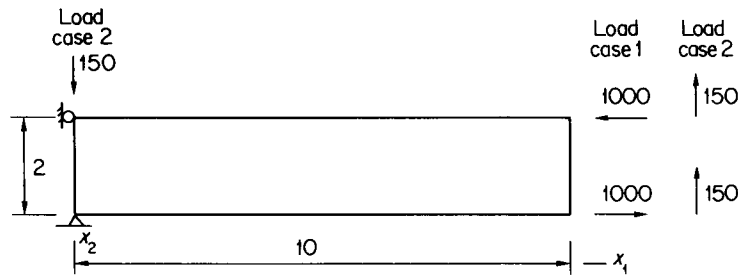
(a) Axial loading results—load case 1

Element	A	B	C	D	E	F	G	H	I
Q4	-0.008	0.399	0.602	1.436	2.271	2.464	2.837	3.071	2.777
Q6	0.002	0.270	-2.414	2.684	-0.153	3.083	3.550	3.009	3.007
QM6	-0.022	0.397	0.539	1.479	2.418	2.555	2.922	3.024	3.000
Q6*	-0.061	0.338	0.028	1.262	2.495	2.808	3.796	3.009	3.007
QM6*	-0.007	0.455	0.454	1.479	2.503	2.498	3.008	3.024	3.000
Exact	0	0.500	0.500	1.500	2.500	2.500	3.000	3.000	3.000

(b) Bending load results—load case 2

Element	$u_1(a)$ —axial	$u_2(a)$ —bending
Q4	6.000	-17.00
Q6	6.701	-19.66
QM6	6.000	-17.61
Exact	6.000	-18.00

(c) Displacements at tip—point a on Figure 2(b)* Results computed at 2×2 Gauss quadrature points and extrapolated using (3) to each stress point.

Figure 3. One element cantilever problem description ($E = 1,500$, $\nu = 0.25$)

should be noted that the stresses are exact at the points considered and for the shear loading the displacements are the best of all the elements considered in Reference 4.

Finally we consider the example shown in Figure 4. This example problem has also been considered in References 3, 4. The properties of the plane stress analysis are $E = 1,500$ and $\nu = \frac{1}{3}$. The dimensions of the body are shown in Figure 4. The results of the analysis for a total shear force of one unit (uniformly distributed along the right edge) are shown in Figure 5 and Table III. These results are comparable to those obtained in Reference 3 for the displacements but superior for the stresses.

Closure

The example problems considered in this note demonstrate the type of results which can be obtained with the QM6 modified incompatible mode element. Similar results have also been obtained for three-dimensional analyses. From the results of the first and second example problems it is evident that QM6 passes all patch tests considered while the original Q6 does not. Thus, one can employ the QM6 element in analysis and be assured that convergence will occur as the mesh is refined even if the limit mesh is not composed of parallelograms. A second observation which can be made is that the element is truly higher order (i.e., of quadratic displacement accuracy) when the mesh is composed of parallelograms only. The last example demonstrates the accuracy of results which can be obtained when applied to typical plane stress problems.

Table II. Results for problem in Figure 3

Element type	Load case	Displacement u_2 at A	Stress at centre of lower edge	
			τ_{11}	τ_{22}
Q4*	1	9.0	289	72
C5L*	1	99.9	3,000	12
C5ML*	1	102.4	3,000	-300
Q6, QM6	1	100.0	3,000	0
Exact	1	100.0	3,000	0
Q4*	2	9.3	217	54
C5L*	2	77.4	2,250	9
C5ML*	2	79.3	2,250	-218
Q6, QM6	2	77.5	2,250	0
Theory	2	102.6	2,250	0

* Results taken from Reference 4.

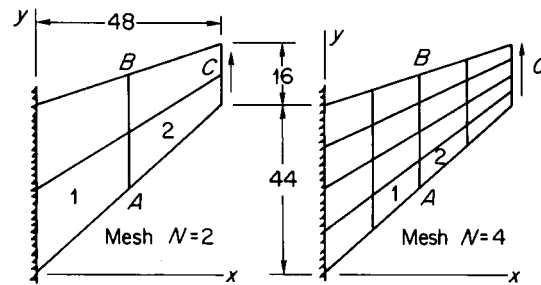
Figure 4. Plane stress structure with unit load uniformly distributed along right edge ($E = 1.0$, $\nu = 1/3$)

Table III. Results for problem shown in Figure 4

Element	u_2 —deflection at C		
	$N = 2$	$N = 4$	$N = 16$
HL*	18.17	22.03	23.81
HG*	22.32	23.23	23.91
Q4*	11.85	18.30	23.43
Q6	22.94	23.48	
QM6	21.05	23.02	
Element	Minimum stress at B		
	$N = 2$	$N = 4$	$N = 16$
HL*	-0.1335	-0.1700	-0.2005
HG*	-0.1394	-0.1566	-0.1952
Q4*	-0.0916	-0.1510	-0.2002
Q6	-0.1936	-0.1936	
QM6	-0.1565	-0.1853	
Q6†	-0.1734	-0.1915	
QM6†	-0.1580	-0.1856	
Element	Maximum stress at A		
	$N = 2$	$N = 4$	$N = 16$
HL*	0.1582	0.1980	0.2294
HG*	0.0933	0.1628	0.2225
Q4*	0.1281	0.1905	0.2358
Q6	0.1866	0.2210	
QM6	0.1900	0.2239	
Q6†	0.2029	0.2258	
QM6†	0.1928	0.2243	

* Results taken from Reference 3.

† Results computed at 2×2 Gauss quadrature points and extrapolated to nodes using (3) for each stress component; nodal stresses are averaged to report a single value.

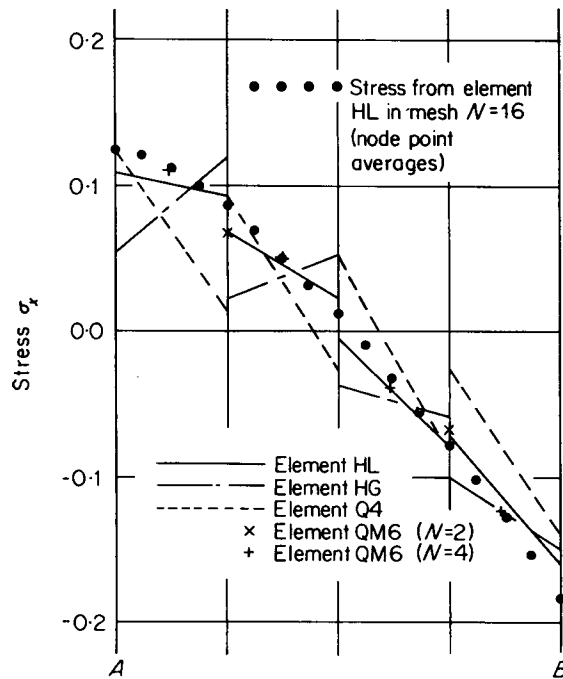


Figure 5. Normal stress along line AB in Figure 4

In closing we must comment on our experiences in attempting to correct the defects in axisymmetric analysis with the Q6 element. First no simple correction can be made since the Q6 element does not capture a constant z normal stress when the radial boundaries are restrained. This implies that more corrections must be made than those discussed above. We have attempted two such corrections and these are discussed and an example problem presented in Reference 5. The most promising method appears to be the one which ignored incompatible modes in computing the hoop strain and then used the method described above to force satisfaction of the patch test.

REFERENCES

1. E. L. Wilson, R. L. Taylor, W. P. Doherty and J. Ghaboussi, 'Incompatible displacement models', in *Numerical and Computer Methods in Structural Mechanics* (Ed. S. J. Fenves, et al), Academic Press, New York, 1973, p. 43.
2. G. Strang and G. J. Fix, *An Analysis of the Finite Element Method*, Prentice-Hall, Englewood Cliffs, N.J., 1973.
3. R. D. Cook, 'Improved two-dimensional finite element', *J. Struct. Div., ASCE*, **100**, ST9, 1851 (1974).
4. R. D. Cook, 'Avoidance of parasitic shear in plane element', *J. Struct. Div., ASCE*, **101**, ST6, 1239 (1975).
5. P. J. Beresford, 'A formulation for non-conforming finite elements', *Master of Science Report 558*, Div. Struct. Engng and Struct. Mech., Univ. of California, Berkeley (1972).